

UC San Diego

UC San Diego Previously Published Works

Title

Contribution of extracellular matrix components to the stiffness of skeletal muscle contractures in patients with cerebral palsy

Permalink

<https://escholarship.org/uc/item/6661w0d4>

Journal

Connective Tissue Research, 62(3)

ISSN

0300-8207

Authors

Smith, Lucas R

Pichika, Rajeswari

Meza, Rachel C

et al.

Publication Date

2021-05-04

DOI

10.1080/03008207.2019.1694011

Peer reviewed



Published in final edited form as:

Connect Tissue Res. 2021 May ; 62(3): 287–298. doi:10.1080/03008207.2019.1694011.

Contribution of extracellular matrix components to the stiffness of skeletal muscle contractures in patients with cerebral palsy

Lucas R. Smith¹, Rajeswari Pichika², Rachel C. Meza^{3,4}, Allison R. Gillies³, Marwan N. Baliki², Henry G. Chambers⁵, Richard L. Lieber^{2,3,6}

¹Departments of Neurobiology, Physiology, and Behavior and Physical Medicine and Rehabilitation, University of California, Davis, CA, 95616, USA

²Shirley Ryan AbilityLab and Department of Physical Medicine and Rehabilitation, Northwestern University, Chicago, IL, 60611, USA

³Department of Orthopaedic Surgery, University of California San Diego, La Jolla, CA, 92093-0863, USA

⁴Department of Biology, University of California San Diego, La Jolla, CA, 92093, USA

⁵Department of Orthopaedics, Rady Children's Hospital, San Diego, CA, USA

⁶Hines V.A. Medical Center, Maywood, IL, USA

Abstract

Joint contractures in children with cerebral palsy contain muscle tissue that is mechanically stiffer with higher collagen content than typically developing children. Interestingly, the correlation between collagen content and stiffness is weak. To date, no data are available on collagen types or other extracellular matrix proteins in these muscles, nor any information regarding their function. Thus, our purpose was to measure specific extracellular protein composition in cerebral palsy and typically developing human muscles along with structural aspects of extracellular matrix architecture to determine the extent to which these explain mechanical properties. Biopsies were collected from children with cerebral palsy undergoing muscle lengthening procedures and typically developing children undergoing anterior cruciate ligament reconstruction. Tissue was prepared for determination of collagen types I, III, IV, and VI, proteoglycan, biglycan, decorin, hyaluronic acid/uronic acid and collagen crosslinking. All collagen types increased in cerebral palsy along with pyridinoline crosslinks, total proteoglycan, and uronic acid. In all cases, type I or total collagen and total proteoglycan were positive predictors, while biglycan was a negative predictor of stiffness. Together these parameters accounted for a greater degree of variance within groups than across groups, demonstrating an altered relationship between extracellular matrix and stiffness with cerebral palsy. Further, stereological analysis revealed a significant increase in collagen fibrils organized in cables and an increased volume fraction of fibroblasts in CP muscle. These data demonstrate a novel adaptation of muscle extracellular matrix in children with cerebral

Corresponding author: Richard L. Lieber Ph.D., Shirley Ryan AbilityLab, 345 East Erie St, Chicago, IL 60611, Phone: (312) 238-6260, rlieber@sralab.org.

DECLARATION OF INTEREST:

None.

palsy that includes alterations in extracellular matrix protein composition and structure related to mechanical function.

Keywords

Cerebral palsy; muscle; collagen; extracellular matrix; stiffness

INTRODUCTION

Cerebral Palsy (CP) represents a spectrum of neuromuscular impairments resulting from damage to the motor cortex. While the central nervous system (CNS) lesion is nonprogressive, the resulting musculoskeletal impairments are indeed progressive and often lead to deforming muscle contractures. Muscle contractures are characterized by increased joint stiffness that limits range of motion, as well as being weaker compared to typically developing (TD) children [1, 2]. Increased stiffness that causes contracture comes from both increased sarcomere strain on the muscle fibers [3, 4] and an intrinsic stiffening of the muscle tissue [2]. When single muscle fibers from patients with CP were examined, they did not have altered stiffness compared to controls, however, when bundles of fibers including their associated ECM were tested stiffness increased in CP [2], strongly implicating the ECM as the source of excessive stiffness in muscle contractures. Yet the structures within the ECM that give rise to the excessive stiffness in muscle contractures are not well understood.

In addition to its role as a cellular scaffold, muscle ECM plays an essential part in transmitting forces produced by the fiber and setting the passive stiffness of the tissue [5, 6]. As in many muscle diseases including muscular dystrophy [7], the muscle ECM in CP is fibrotic with dramatic accumulation of collagen [2, 8]. Fibrillar collagen is known as the primary tensile load bearing element within the ECM [9] and tissue stiffness scales with collagen expression over multiple order of magnitude [10]. However, intriguingly, total collagen content is only weakly correlated with elastic stiffness of fibrotic muscle tissue from the lower limb [see Figure 3 of reference 11]. Further, muscle from contracture in CP demonstrates a variety of altered ECM components beyond only collagen [12, 13]. Therefore, we hypothesized that other ECM components, which are capable of bearing load within the ECM or modifying fibrillar collagens, might explain variation in stiffness of muscles in contracture.

The most common structural proteins in muscle ECM are collagens, proteoglycans and associated glycosaminoglycans. Collagen has over 25 known isoforms, comprising both fibrillar and laminar structures. Type I (fibrillar) is by far the most common isoform and is associated with high tissue stiffness [14]. Type III is the next most common fibrillar form and is associated with high tissue compliance [15, 16]. Type IV is the most common laminar type and dominates the basement membrane while Type VI provides a linkage between the basement membrane and the interstitial matrix. Mutations in Type VI collagen are associated with a range of muscle pathologies, potentially mediated through a role supporting satellite cell based muscle regeneration [17]. All isoforms have the same basic triple helix structure

with variations in sequence and length, contributing to their different functionalities. Collagens undergo extensive post-translational modification, including the formation of intra- and intermolecular collagen crosslinks that strengthen and stiffen collagen networks [18]. Higher order structure of collagen molecules including the fiber size, length, and orientation can also influence mechanical properties [19]. While these structures are difficult to quantify in composite tissue such as muscle, a new methodology combining stereology with serial block face scanning electron microscopy allows direct visualization and quantification of collagen fibrils within tissue.

The ECM also includes abundant glycoproteins, with proteoglycans that have formed glycosaminoglycan (GAG) chains. They have a diverse collection of roles, ranging from extracellular support to regulation of molecular movement through the ECM. Their major biomechanical function serves to hydrate and maintain ECM viscoelastic properties [20]. Proteoglycans with a smaller core protein are known as small leucine-rich proteoglycans (SLRPs) and include decorin and biglycan. The SLRPs role in determining stiffness likely relates to their interactions with collagens [21]. For instance, decorin aids in fibrillar collagen formation (Types I and III) and may influence fibrillogenesis [22] and both influence collagen fibril structure within tissue [21, 23]. Yet, there are no reports of alterations of glycoproteins in muscle contracture.

Unfortunately, no previous studies have extensively quantified muscle ECM components that play major passive load-bearing roles in muscles from patients with CP [24]. The semitendinosus of the medial hamstring was studied here based on the prevalence of knee flexion contractures in children with CP [25] and for consistency with earlier studies [2]. Given the biomechanical changes measured in contractured muscle, its hypertrophic ECM, and the potential roles of many ECM proteins in load bearing, the purpose of this study was to quantify the ECM components in CP and TD muscles and determine the extent to which any of these proteins scale with measured mechanical properties. Knowledge of the nature of ECM remodeling's contribution to stiffness in muscle contractures may lead to future treatment strategies for patients with CP.

MATERIALS AND METHODS

Muscle biopsy collection

Ethical approval for this study conformed to the standards of the Declaration of Helsinki and was approved by the Institutional Review Board of University of California, San Diego and Northwestern University Human Research Protection Programs. After obtaining consent from parents and age appropriate assent from children, semitendinosus (ST) muscle biopsies were collected from children with cerebral palsy (CP) ($n=13$, mean age 10.4 ± 4.4 years) undergoing tendon lengthening procedures and typically developing (TD) children ($n=13$, mean age 15.5 ± 2.0 years) undergoing anterior cruciate ligament reconstruction with hamstring autograft. All TD children had no history of a neurological disorder. The surgical procedures both accessed the muscle at the extreme distal end of the semitendinosus so there was minimal variability between biopsy sites. Prior to preserving the biopsy any visually apparent pieces of tendon, aponeurotic extensions, or fat was removed from the muscle tissue. Passive mechanic data from these children was previously published and was used as

the dependent variable for regression analyses [2]. All muscle biopsies were stored at -80°C . Prior to biochemical assays, tissue was homogenized by pulverizing into a fine powder on liquid nitrogen using a Cryopress (Microtech, Japan).

Solubilization of Collagens

Approximately 20 mg of the powdered tissue was digested with 4M guanidine hydrochloride (Sigma Chemicals, St. Louis, MO) for 4h with proteases inhibitors at 4°C . The digested sample was desalted using slide-A-Lyzer (Pierce, IL). Biglycan, decorin and hyaluronic acid (HA) were quantified using ELISA kits (Antibodies-online, GA). Powdered tissue was homogenized with 2.0 ml of phosphate-buffered saline containing protease inhibitors (Roche Diagnostics, IN) and snap frozen. To quantify collagen types, inter- and intramolecular collagen crosslinks were solubilized with pepsin (100 $\mu\text{g}/\text{ml}$, Sigma, MO) in 0.05M acetic acid overnight at 4°C , followed by 1 mg/ml elastase for 4 hrs at 4°C to remove elastic fibers, and then neutralized with 5N NaOH. Neutralized samples were analyzed by enzyme linked immunosorbent assay (ELISA) and collagen types were quantified using antibodies against chains Ia1, IIIa1 (Chondrex, Redmond, WA), IVa1 (My BioSource, CA), and VIa2 (My BioSource, CA).

Collagen Crosslinks by High Performance Liquid Chromatography (HPLC)

Muscle biopsies (10 mg) were hydrolyzed with 6N HCl at 110°C for 20 h in a sealed tube to prevent evaporation. The hydrolysates were dried in a stream of nitrogen gas. Dried samples were dissolved in 95 μL water (containing 10 nmol pyridoxine hydrochloride/ml as internal control) per mg tissue and then purified using 0.22 μm Spin-X centrifuge tube filters (Costar, Corning, NY). Hydroxyllysyl pyridinoline (HP), lysyl pyridinoline (LP), and pentosidine (PE) concentrations of the semitendinosus samples were determined as previously described [26] with slight modification. Samples were diluted four-fold with 0.5% (v/v) heptafluorobutyric acid (HFBA) in 10% (v/v) acetonitrile. The samples (50 μL) were injected into HPLC system (Shimadzu, IL). The HPLC column (TSK gel ODS-80T_m, 4.6 mm I.D. x 15 cm) packed with 5 μm particles (TOSOH Bioscience, Japan) was first equilibrated with 0.15% (v/v) HFBA in 24% (v/v) methanol (eluent A). Elution of crosslinks and pyridoxine internal standard was achieved at 40°C at a flow rate of 1.0 mL/min in two isocratic steps. From 0–17 minutes, eluent A was used, and from 17–30 min 0.05% (v/v) HFBA in 40% (v/v) methanol (eluent B) was used. The column was then washed with 0.1% (v/v) HFBA in 75% (v/v) acetonitrile (eluent C) for 10 min and equilibrated for 10 min using 0.15% (v/v) HFBA in 24% (v/v) methanol. Fluorescence was monitored at 295/400 nm from 0–22 min and 328/378 nm (gain 100; band width 18 nm) from 22–45 min. Quantification of HP, LP and PE was achieved by external calibration using pyridinoline (PYD) and deoxypyridinoline (DPYD) standards (Quidel, San Diego). Elution of HP occurred at 9.8 minutes, LP at 12.1 minutes, and PE at 21.5 minutes.

Hydroxyproline Assay by HPLC

For hydroxyproline analyses, 20 μL of the diluted sample and hydroxyl L-proline standard were dried and incubated for 10 min at room temperature with 20 μL of derivatization solution [methanol:water:trimethylamine:phenylisothiocyanate (7:1:1:1)]. Lyophilized hydroxy-L-proline (20 $\mu\text{g}/\text{ml}$) and samples were dissolved in 100 μL of reconstitution buffer

(5mM Na₂HPO₄ in acetonitrile at pH 7.4). Samples (50 µL) were injected in the HPLC system using an auto sampler. Hydroxyproline content was determined using an HPLC column (Waters Spherisorb ODS-80. 4.6 mm I.D. x 25 cm 2–5 µm particles, All Tech, IL) equilibrated with a 6:4:90 solution of acetonitrile:water:140 mM sodium acetate trihydrate buffer, pH 6.4 for 15 min at a flow rate of 1 ml/min. Elution of hydroxyproline occurred at 9 minutes. At 13 min, the column was washed with 60% acetonitrile. Fluorescence was monitored at 254 nm. The concentration of the unknown sample was created using a standard curve derived from the commercially available standard hydroxy L- proline.

Determination of Proteoglycan and Glycosaminoglycan Content

Approximately 10 mg of muscle biopsies were digested at 56°C using papain in phosphate buffer (0.25 g/10 ml at pH 6.5, with cysteine at 0.078 g/10 ml). After digestion, 10 µL of the sample was analyzed for proteoglycan content [27]. Briefly, 10 µL of the digested sample was diluted to 40 µL with phosphate buffer followed by addition of 250 µL of 1, 9-dimethylmethylene blue (21 µg/ml) pH 1.5. The concentration of proteoglycans was measured using bovine chondroitin sulfate (CS) as a standard. Absorbance was read at 530 nm/595 nm using a microplate reader (Synergy HT1, BioTek, VT). Uronic acid was measured by the method described in reference [28]. Briefly, serial dilutions of standard D-glucuronic acid lactone and papain-digested samples were placed in 96 well plates. Then, 200 µL of 25 mM sodium tetra borate in sulfuric acid was added. The plate was heated for 10 min at 100°C in an oven. After cooling at room temperature for 15 min and addition of 0.125% carbazole in absolute ethanol, the absorbance was measured at a wavelength of 550 nm.

Stereological Analysis and Imaging

Volume fractions of ECM components were measured from transmission electron micrographs prepared as previously described and implemented in an animal model of skeletal muscle fibrosis [29] using approximately 50 mg of a preserved intact muscle biopsy. Briefly, transmission electron micrographs for stereological analysis were acquired using a multi-stage sampling scheme. After biopsy fixation and embedding, one section from each tissue block was imaged (n = 5 blocks per muscle, n = 13 muscles). Micrographs were obtained from two serial sections per block, and each section was divided into four random fields of view to be imaged at low and high magnification. Based on the stereology point sampling density (see example in Fig. 5A), this yielded a total of 441 data points per section and 17,640 data points per specimen. Images were analyzed with IMOD software using the stereology plug-in [30]. A 20 × 20 square grid (grid spacing 0.79 µm, 400 points/grid) was overlaid on each low magnification micrograph and each point was classified as myofibril, mitochondria, myonucleus, satellite cell, fibroblast, extracellular space, nerve, capillary, or other by a trained technician. Cell classifications were based on histology atlases and references [31, 32]. To quantify objects within the extracellular space, 27 × 27 square grids (grid spacing 85.6 nm, 729 points/grid) were overlaid on high magnification micrographs and points within the extracellular space were classified as interstitial space (no visible object), single collagen fibril, collagen fibril in cable, or basal lamina. Point counts were summed for each specimen and volume fractions of myofibrils, mitochondria, myonuclei, satellite cells, fibroblasts, extracellular space, nerves, and capillaries were defined as the

total object point count divided by the total number of points counted at low magnification. Volume fractions for single collagen fibril, collagen fibrils in cable, and basal lamina in the muscle, V_{col}/V_M , were calculated using the following equation:

$$\frac{V_{col}}{V_M} = \left(\frac{V_{col}}{V_s}\right)\left(\frac{V_s}{V_M}\right) \quad (1)$$

where V_{col}/V_s is the fraction of collagen (single fibril, fibril in cable, or basal lamina) in the extracellular space calculated at high magnification and V_s/V_M is the fraction of extracellular space in the muscle calculated at low magnification. Overall, this sampling approach measured a total of 845 images at 1,650x and 11,000x magnifications.

Transcriptional analysis from GEO Datasets

Transcriptional data from a previously published work [13] on the GEO datasets website (GSE31243) was analyzed for individual ECM genes. The biopsies come from a highly similar patient population as the current study, undergoing the same surgeries for both TD and CP and accessing the same portion of the semitendinosus. When multiple spots microarray IDs were available for a single gene, only the ID with the highest average value among all samples was analyzed. For collagen genes that contain multiple α -chains, only the α -chain gene with the highest average expression among all samples was analyzed.

Statistical Analyses

Two-way ANOVA was used to compare dependent variables between CP and TD groups and different ECM types with a post-hoc Sidak test for individual component differences between CP and TD. Multiple stepwise regression was used to determine which proteins, if any, correlated with muscle fiber bundle stiffness. R^2 -to-Enter was set to 0.08 and R^2 -to-Remove was set to 0.05. Critical significance level was set to $\alpha=0.05$ and error bars represent standard error of the mean.

RESULTS

In agreement with previous reports [2, 33], fiber bundles from patients with CP demonstrated an approximately 50% increase in stiffness compared to semitendinosus biopsies of TD children (Fig. 1A). Also consistent with previous studies was the five-fold increase in collagen as measured by hydroxyproline content (Fig. 1B). The fibrillar collagens I and III, basal lamina collagen IV, and interstitial collagen VI measured by ELISA all showed similar 3–5 fold significant increases in CP patients (n=13) compared to TD children (n=13) (Fig. 2A). The ratio of collagen I to collagen III, which decreases in scar and wound healing, trended down in CP, but was not significantly different between groups (Fig. 2B). Collagen I was by far the most prominent collagen studied, accounting for ~70% of total collagen, followed by types IV, III, and VI, however, there was not a consistent change in the proportion of different collagens between TD and CP patients (Fig. 2C). The physical properties of collagen are modulated by the presence of inter- and intramolecular crosslinks. Hydroxylysyl (HP) and lysyl-pyridinoline (LP) are enzymatically initiated mature crosslinks that enhance collagen stability and stiffness [34], while advanced glycation end-products (AGEs) form as a result of exposure to sugars with pentosidine as a

biomarker of age [35]. Consistent with pyridinoline crosslinks being a marker of fibrosis [36], both types of crosslinks were significantly increased in CP while pentosidine remained unaffected in CP muscle (Sup. Fig. 1).

ECM components beyond collagen can impact matrix stiffness, particularly glycosaminoglycans (GAG) and associated proteoglycans. GAGs contain uronic acid and an acetylated sugar repeat and play roles in matrix hydration as well as collagen interactions. Total uronic acid was significantly increased in patients with CP, although hyaluronic acid, a GAG associated with muscle regeneration [37], was not significantly different between patient groups (Fig. 3A). Overall, the amount of proteoglycans containing GAGs were unchanged in CP (Fig. 3B). Surprisingly, individual SLRPs were distinctly regulated with decorin increasing and biglycan decreasing in CP, despite their largely similar functions [38]. The distinct regulation of SLRPs does not appear to be at the transcriptional level, as analysis of similar transcriptional datasets from CP and TD populations show no change in transcripts for enzymes related to hyaluronic acid synthesis or breakdown of decorin. Surprisingly, there was a significant increase in biglycan gene transcription that was in the opposite direction as the protein expression (Sup. Fig. 2A) [13]. This result is in contrast to the expression of collagen genes that correlated well with protein data showing significant increases for all collagen (Sup. Fig. 2A).

This study produced the most detailed descriptions of the biochemical makeup of CP ECM in precisely the same samples that were mechanically tested. This allows quantitative investigation of which ECM components contribute to stiffness by stepwise linear regression. Analysis of all 26 samples containing 14 biochemical measures of the ECM resulted in a model that was able to account for 65% of the variance observed in muscle tissue stiffness (Fig 4A). The model incorporated collagen I and total proteoglycan as positive predictors of stiffness and collagen III and biglycan as negative predictors of stiffness, with biglycan accounting for the highest degree of variance at 28% (equations at the bottom of Fig. 4). This slightly counterintuitive result and the rather modest fit can be explained by the distinct relationships between stiffness and ECM components from TD vs. CP muscles. For example, collagen I and bundle stiffness are both higher in CP leading to a highly significant correlation between type I collagen content and stiffness, however within the CP or TD group the association is neither strong, nor significant (Sup. Fig. 3A). This is even more pronounced with hydroxyproline in which there is no overlap between TD and CP that results in a highly significant correlation overall, yet within the TD population the positive correlation is completely lost (Sup. Fig. 3B). Biglycan showed a negative correlation with stiffness when both groups were combined, but has no correlation with each group separately (Sup. Fig. 3C). These results illustrate the fact that significant correlations break down when the individual groups are considered separately simply because of the differences between groups. However, the opposite case also occurs—insignificant correlations become significant when the individual groups are considered separately. Specifically, the collagen I/III ratio is not significant when considering both groups together, but is highly significant when considering only the CP samples (Sup. Fig. 3D). When regression is performed on individual groups the amount of variance and the overall significance of the fit is greatly enhanced, accounting for 84% of variance for TD and 89% of variance in CP (Fig. 4B). In CP muscle, the collagen I/III ratio accounted for over half the

variance (Sup. Fig. 4) with positive relationships to proteoglycan and hydroxyproline and a negative correlation to biglycan. For TD muscles there was a positive relationship with HP crosslinks, collagen I, collagen IV and proteoglycan, while the negative correlation to biglycan remained. Thus, while the contribution of proteoglycan and biglycan to stiffness remained nearly unchanged by the disease state, the muscle in CP lost its dependence on collagen types I and IV and crosslinking and replaced it largely with collagen I/III ratio. The inability of one single regression model to explain muscle mechanical properties for both experimental groups strongly suggests that these ECM components may not directly relate to stiffness, rather are part of the muscle programs that control stiffness and those programs are distinct for muscles from typically developing children or those with cerebral palsy. This was clearly observed when observing the correlation matrix of all parameters. For TD muscle, the collagens clearly clustered as did proteoglycans (Sup. Fig. 5A), but this relationship was lost in CP muscle (Sup. Fig. 5C). Across the matrix the average correlation coefficient was 0.28 for TD (Sup. Fig. 5B), but was only 0.07 for CP (Sup. Fig. 5D).

Beyond just the biochemical content of ECM components, the structural manner in which they are arranged can have a critical impact on their contribution to resistance to unilateral stretch [39]. Stereology performed on transmission electron micrographs allows for the quantification of structural components in tissues (Fig. 5A), including assessment of the ECM. Unsurprisingly, regardless of disease state ~80% of the muscle consists of contractile myofibrils (Fig. 5B). However, in CP there was a significant increase in the amount of collagen fibrils visible in collagen cables (Sup. Fig. 6), while the amount of collagen in isolated single fibrils remained unchanged in CP. This demonstrates a change that occurs in collagen organization that is undetectable by biochemical analysis. The basal lamina volume fraction was unchanged in cerebral palsy, along with the volume of mitochondria, myonuclei, blood vessels, and, somewhat surprisingly satellite cells [40, 41]. Along with the increase in collagen cables, fibroblasts, which are responsible for secreting ECM and contribute to ECM organization, were also more prolific in CP compared to TD as reflected by an increase in volume fraction of fibroblasts. Unfortunately stereological samples were distinct from the mechanically tested specimens for technical reasons, but these data suggest an intriguing possibility of a direct relationship between ECM architecture and the stiffness of muscle that causes debilitating contractures in patients with cerebral palsy.

DISCUSSION

The development of joint contractures in patients with cerebral palsy is highly disabling and current treatments have limited efficacy. The increased passive stiffness of skeletal muscle leads to contracture formation in CP [33] yet our understanding of the structures responsible for the enhanced passive stiffness of muscle is incomplete. One structural change that is repeatedly observed is increased muscle strain results in long sarcomeres that extend muscle further along the length tension curve, limiting active force generation and increases stiffness [3, 4]. However, several publications have documented intrinsically stiffer muscle [2, 42–44] as observed in the current study. It is feasible that muscle fibers themselves become stiffer in CP [42, 45], however, previous studies on the semitendinosus (also reported here Fig. 1A) or gracilis show no change in myofiber stiffness and either no [2], or minimal [46] changes in titin isoform responsible for establishing myofibrillar stiffness [47].

Alternatively, the ECM has been shown to undergo drastic changes in muscle contractures [2, 8] and is the dominant source of passive tension in many tissues [10]. Here we have conducted a detailed study of the ECM proteins present in contractured or healthy muscle and describe novel relationships among these ECM proteins and muscle tissue (bundle) stiffness. It is important to note that contractures are progressive and thus the ECM stiffness along the associated ECM content and architecture are also expected to progress with time and may be distinct in adult populations. Longitudinal studies are required to provide valuable insights into this relationship but are not currently feasible due the invasive method needed to acquire tissue.

Collagens were the primary focus of the study, as they are known to be the primary load bearing structures within the ECM [9]. Muscles from patients with CP had dramatically increased collagen content overall, consistent with previous studies on ECM of muscle in CP (Fig. 1B) [2, 8]. Each of the individually measured collagen types showed a persistent 3–5 fold increase in CP indicating proliferation of both the interstitial matrix and the basal lamina (Fig. 2). Collagen I was the predominant collagen measured and correlated well with overall hydroxyproline content ($r^2 = 0.80$). Both TD (collagen I) and CP (hydroxyproline), as well as the combined model (collagen I), use these parameters as positive predictors of muscle stiffness. However, these measures account for only ~10% of the variance in the overall stiffness (Fig. 4, Sup. Fig. 4), clearly indicating other structures or higher order of structure play an important role in determining stiffness. Other collagen isoforms appeared in the model as well, with collagen IV being a surprising positive predictor of stiffness in TD muscle. This may relate to the role of the basal lamina in confining the area of myofibers rather than creation of an actual tensile load along the muscle fiber axis [48]. On the other hand, despite being a major fibrillar collagen, collagen III was a negative predictor of muscle stiffness overall. This is consistent with incorporation of collagen III leading to a decrease in stiffness of collagen fibrils [49] and collagen III increasing tissue compliance [15, 16]. However, there was a trend for collagen I/III ratio to decrease in CP as is observed in other fibrotic conditions [50] and that ratio was the first parameter to enter the model in CP, accounting for a majority of the variance (56%). This evidence supports the idea that in cerebral palsy collagen regulation is altered in such a manner that all collagens increase, but with a program that produces a decreased collagen I/III ratio. While tissue stiffening does not directly result from increased relative collagen III, it may be a consequence of the same ECM regulatory process.

The mechanical properties of a collagen network are defined by more than just its constituent parts, but also the organization of the collagen matrix. The most readily studied aspect of organization is collagen crosslinking, which enhances stability and tensile stiffness of collagen [18]. In CP, the enzymatic pyridinoline crosslinks were highly increased while the AGE crosslinks were unaltered (Sup. Fig. 1). The enhanced crosslinking in CP aligned with the increased stiffness in CP, however, only in TD were HP crosslinks a positive predictor of stiffness (Fig. 4). Notably, LP crosslinks did enter the model for CP, but were subsequently removed based on covariance with other parameters. Pyridinoline crosslinks increased significantly (2–3 fold), but not to the same degree as collagens such that crosslinks per collagen molecule were decreased in CP. This may explain the increase in intrinsic stiffness of the muscle in contracture being less than that of the increase in matrix

constituents. Previous investigation of crosslinking in mouse models of muscle fibrosis showed little relationship between crosslinking and muscle stiffness [51], consistent with the current study.

Apart from their mechanical role, collagen crosslinks reduce susceptibility to proteolytic cleavage of the matrix and ECM turnover [52], however activity of collagen proteases may be mitigated by applying tensile load to collagen [53]. This mechanism may connect the enhanced strain observed in muscle contracture to the increase in ECM components, particularly as collagen protein content was more highly upregulated in CP compared to transcriptional activity. In skeletal muscle, the external tensile load is applied uniaxially in the direction of the fibers and in general the collagen cables that extend beside them [5]. This architecture positions collagen perimysial cables as a potential major load bearing structure within ECM. The presence of these collagen cables within the ECM can be measured stereologically using transmission electron microscopy [29]. While it is unfortunate that mechanical measurements were not available for these samples, the presence of collagen fibrils organized into cables was significantly increased in CP (Fig. 5), along with an increase in fibroblasts that are closely associated with them [55]. Meanwhile the volume of isolated collagen fibrils and basal lamina remained unchanged. This suggests the intriguing possibility that higher order structures may determine tissue stiffness to a greater extent than molecular components; however, further studies are needed to establish such a connection as well as their potential covariance with ECM components.

Beyond collagen, proteoglycans make up an important constituent of the ECM in muscle and are correspondingly upregulated in fibrotic conditions (Fig. 3) [56, 57]. In addition to their vital role in modulating cell signaling molecule availability, proteoglycans directly influence mechanics by controlling hydration state to modulate hydrodynamic pressure [20]. In both TD and CP groups, total proteoglycan content was a positive predictor of bundle stiffness (Fig. 4). Proteoglycans also interact with collagen and have an important role in collagen fibril assembly, particularly the SLRPs decorin and biglycan [58]. Interestingly, while decorin scaled generally with total proteoglycan, biglycan was inversely related to total proteoglycan and thus significantly decreased in CP. Despite their similar function, differential regulation of decorin and biglycan has been observed in response to retinoic acid [59] and in some instances of muscular dystrophy [60]. Biglycan, independent of proteoglycan, was one of the best predictors of bundle stiffness, with a negative relationship in each group. In skeletal muscle, biglycan has been shown to play an important role in neuromuscular junction stability [61], which may be disrupted in CP [62]. Administration of recombinant biglycan has actually been shown to alleviate the dystrophic condition in mouse models [63] and may thus present a potential therapy in CP. We do not propose a direct mechanical role for biglycan or decorin, but these data reflect the synthetic activity of the SLRPs in skeletal muscle.

These data provide a detailed investigation of the altered ECM composition and structure in muscle from patients with CP compared to TD patients and their relationship to muscle tissue stiffness. All isoforms of collagen were increased in CP and associated with tissue stiffness, however in CP, the collagen I/III ratio was the critical predictor of stiffness. This alteration was not well associated with levels of collagen crosslinking; however, further

exploration of collagen cable formation may elucidate currently unknown mechanical relationships. Our evidence showed that total proteoglycan content supports tissue stiffness, yet the decrease in biglycan in CP was inversely related to stiffness. These data emphasize that ECM components, including fibrillar collagens, are critical in determining stiffness and highlight potential negative regulators (biglycan) that may play a therapeutic role in increasing muscle compliance in contractures of patients with cerebral palsy and potentially other fibrotic muscle disorders.

Supplementary Material

Refer to Web version on PubMed Central for supplementary material.

ACKNOWLEDGEMENTS

We thank Dr. Jess Snedeker for his valuable discussions. We also acknowledge the donors and their families who provided consent for the biopsies. This work was supported in part by Research Career Scientist Award Number IK6 RX003351 from the United States (U.S.) Department of Veterans Affairs Rehabilitation R&D (Rehab RD) Service.

FUNDING:

This work was supported by grant from the National Institute of Health P30AR061303 and AR057393.

REFERENCES

1. Elder GC, et al., Contributing factors to muscle weakness in children with cerebral palsy. *Dev Med Child Neurol*, 2003. 45(8): p. 542–50. [PubMed: 12882533]
2. Smith LR, et al., Hamstring contractures in children with spastic cerebral palsy result from a stiffer extracellular matrix and increased in vivo sarcomere length. *J Physiol*, 2011. 589(Pt 10): p. 2625–39. [PubMed: 21486759]
3. Lieber RL and Friden J, Spasticity causes a fundamental rearrangement of muscle-joint interaction. *Muscle Nerve*, 2002. 25(2): p. 265–70. [PubMed: 11870696]
4. Pontén E, Gantelius S, and Lieber RL, Intraoperative muscle measurements reveal a relationship between contracture formation and muscle remodeling. *Muscle Nerve*, 2007. 36(1): p. 47–54. [PubMed: 17410593]
5. Gillies AM and Lieber RL, Structure and function of the skeletal muscle extracellular matrix. *Muscle and Nerve*, 2011. 44: p. 318–331. [PubMed: 21949456]
6. Meyer G and Lieber RL, Muscle fibers bear a larger fraction of passive muscle tension in frogs compared with mice. *J Exp Biol*, 2018. 221(Pt 22).
7. Smith LR and Barton ER, Regulation of fibrosis in muscular dystrophy. *Matrix Biol*, 2018. 68–69: p. 602–615.
8. Booth CM, Cortina-Borja MJ, and Theologis TN, Collagen accumulation in muscles of children with cerebral palsy and correlation with severity of spasticity. *Dev Med Child Neurol*, 2001. 43(5): p. 314–20. [PubMed: 11368484]
9. Muiznieks LD and Keeley FW, Molecular assembly and mechanical properties of the extracellular matrix: A fibrous protein perspective. *Biochim Biophys Acta*, 2013. 1832(7): p. 866–75. [PubMed: 23220448]
10. Swift J, et al., Nuclear lamin-A scales with tissue stiffness and enhances matrix-directed differentiation. *Science*, 2013. 341(6149): p. 1240104. [PubMed: 23990565]
11. Lieber RL and Ward SR, Cellular mechanisms of tissue fibrosis. 4. Structural and functional consequences of skeletal muscle fibrosis. *Am J Physiol Cell Physiol*, 2013. 305(3): p. C241–52. [PubMed: 23761627]

12. Smith LR, et al., Novel transcriptional profile in wrist muscles from cerebral palsy patients. *BMC Med Genomics*, 2009. 2: p. 44. [PubMed: 19602279]
13. Smith LR, et al., Transcriptional abnormalities of hamstring muscle contractures in children with cerebral palsy. *PLoS One*, 2012. 7(8): p. e40686. [PubMed: 22956992]
14. Gelse K, Poschl E, and Aigner T, Collagens--structure, function, and biosynthesis. *Adv Drug Deliv Rev*, 2003. 55(12): p. 1531-46. [PubMed: 14623400]
15. Miller TA, et al., Hindlimb unloading induces a collagen isoform shift in the soleus muscle of the rat. *Am J Physiol Regul Integr Comp Physiol*, 2001. 281(5): p. R1710-7. [PubMed: 11641144]
16. von der Mark K, et al., Relationship between cell shape and type of collagen synthesised as chondrocytes lose their cartilage phenotype in culture. *Nature*, 1977. 267(5611): p. 531-2. [PubMed: 559947]
17. Urciuolo A, et al., Collagen VI regulates satellite cell self-renewal and muscle regeneration. *Nat Commun*, 2013. 4: p. 1964. [PubMed: 23743995]
18. Lopez B, et al., Collagen cross-linking but not collagen amount associates with elevated filling pressures in hypertensive patients with stage C heart failure: potential role of lysyl oxidase. *Hypertension*, 2012. 60(3): p. 677-83. [PubMed: 22824984]
19. Roeder BA, et al., Tensile mechanical properties of three-dimensional type I collagen extracellular matrices with varied microstructure. *J Biomech Eng*, 2002. 124(2): p. 214-22. [PubMed: 12002131]
20. Yanagishita M, Function of proteoglycans in the extracellular matrix. *Acta Pathol Jpn*, 1993. 43(6): p. 283-93. [PubMed: 8346704]
21. Robinson KA, et al., Decorin and biglycan are necessary for maintaining collagen fibril structure, fiber realignment, and mechanical properties of mature tendons. *Matrix Biol*, 2017. 64: p. 81-93. [PubMed: 28882761]
22. Vogel KG, Paulsson M, and Heinegard D, Specific inhibition of type I and type II collagen fibrillogenesis by the small proteoglycan of tendon. *Biochem J*, 1984. 223(3): p. 587-97. [PubMed: 6439184]
23. Corsi A, et al., Phenotypic effects of biglycan deficiency are linked to collagen fibril abnormalities, are synergized by decorin deficiency, and mimic Ehlers-Danlos-like changes in bone and other connective tissues. *J Bone Miner Res*, 2002. 17(7): p. 1180-9. [PubMed: 12102052]
24. Bank RA, et al., Sensitive fluorimetric quantitation of pyridinium and pentosidine crosslinks in biological samples in a single high-performance liquid chromatographic run. *J Chromatogr B Biomed Sci Appl*, 1997. 703(1-2): p. 37-44. [PubMed: 9448060]
25. Cloudt E, Rosenblad A, and Rodby-Bousquet E, Demographic and modifiable factors associated with knee contracture in children with cerebral palsy. *Dev Med Child Neurol*, 2018. 60(4): p. 391-396. [PubMed: 29318610]
26. Farndale RW, Buttle DJ, and Barrett AJ, Improved quantitation and discrimination of sulphated glycosaminoglycans by use of dimethylmethylene blue. *Biochim Biophys Acta*, 1986. 883(2): p. 173-7. [PubMed: 3091074]
27. Cesaretti M, et al., A 96-well assay for uronic acid carbazole reaction. *Carbohydrate Polymers*, 2003. 54(1): p. 59.
28. Kremer JR, Mastrorade DN, and McIntosh JR, Computer visualization of three-dimensional image data using IMOD. *J Struct Biol*, 1996. 116: p. 71-76. [PubMed: 8742726]
29. Gillies AR, et al., High resolution three-dimensional reconstruction of fibrotic skeletal muscle extracellular matrix. *J Physiol*, 2017. 595(4): p. 1159-1171. [PubMed: 27859324]
30. Scott SH, Engstrom CM, and Loeb GE, Morphometry of human thigh muscles. Determination of fascicle architecture by magnetic resonance imaging. *Journal of Anatomy*, 1993. 182: p. 249-257. [PubMed: 8376199]
31. Carpenter S and Karpati G, Pathology of skeletal muscle. 2001, New York: Oxford University Press.
32. Matuszewski PE, et al., Regional variation in human supraspinatus tendon proteoglycans: decorin, biglycan, and aggrecan. *Connect Tissue Res*, 2012. 53(5): p. 343-8. [PubMed: 22329809]
33. Mathewson MA and Lieber RL, Pathophysiology of Muscle Contractures in Cerebral Palsy. *Phys Med Rehabil Clin N Am*, 2015. 26(1): p. 57-67. [PubMed: 25479779]

34. Oxlund H, et al., Reduced concentrations of collagen cross-links are associated with reduced strength of bone. *Bone*, 1995. 17(4 Suppl): p. 365S–371S. [PubMed: 8579939]
35. Miyata T, et al., Renal catabolism of advanced glycation end products: the fate of pentosidine. *Kidney Int*, 1998. 53(2): p. 416–22. [PubMed: 9461101]
36. van der Slot AJ, et al., Increased formation of pyridinoline cross-links due to higher telopeptide lysyl hydroxylase levels is a general fibrotic phenomenon. *Matrix Biol*, 2004. 23(4): p. 251–7. [PubMed: 15296939]
37. Calve S, et al., Hyaluronic acid, HAS1, and HAS2 are significantly upregulated during muscle hypertrophy. *Am J Physiol Cell Physiol*, 2012. 303(5): p. C577–88. [PubMed: 22785117]
38. Halper J, Proteoglycans and diseases of soft tissues. *Adv Exp Med Biol*, 2014. 802: p. 49–58. [PubMed: 24443020]
39. Taufalele PV, et al., Fiber alignment drives changes in architectural and mechanical features in collagen matrices. *PLoS One*, 2019. 14(5): p. e0216537. [PubMed: 31091287]
40. Smith LR, Chambers HG, and Lieber RL, Reduced satellite cell population may lead to contractures in children with cerebral palsy. *Dev Med Child Neurol*, 2013. 55(3): p. 264–70. [PubMed: 23210987]
41. Dayanidhi S, et al., Reduced satellite cell number in situ in muscular contractures from children with cerebral palsy. *J Orthop Res*, 2015. 33(7): p. 1039–45. [PubMed: 25732238]
42. Mathewson MA, et al., Stiff muscle fibers in calf muscles of patients with cerebral palsy lead to high passive muscle stiffness. *J Orthop Res*, 2014. 32(12): p. 1667–74. [PubMed: 25138654]
43. Alhusaini AA, et al., Mechanical properties of the plantarflexor musculotendinous unit during passive dorsiflexion in children with cerebral palsy compared with typically developing children. *Dev Med Child Neurol*, 2010. 52(6): p. e101–6. [PubMed: 20132139]
44. Brandenburg JE, et al., Quantifying passive muscle stiffness in children with and without cerebral palsy using ultrasound shear wave elastography. *Dev Med Child Neurol*, 2016. 58(12): p. 1288–1294. [PubMed: 27374483]
45. Fridén J and Lieber RL, Spastic muscle cells are shorter and stiffer than normal cells. *Muscle Nerve*, 2003. 27(2): p. 157–64. [PubMed: 12548522]
46. Larkin-Kaiser KA, et al., Relationship of muscle morphology to hip displacement in cerebral palsy: a pilot study investigating changes intrinsic to the sarcomere. *J Orthop Surg Res*, 2019. 14(1): p. 187. [PubMed: 31227002]
47. Brynnel A, et al., Downsizing the molecular spring of the giant protein titin reveals that skeletal muscle titin determines passive stiffness and drives longitudinal hypertrophy. *Elife*, 2018. 7.
48. Smith LR, Gerace-Fowler L, and Lieber RL, Muscle extracellular matrix applies a transverse stress on fibers with axial strain. *Journal of Biomechanics*, 2011. 44(8): p. 1618–20. [PubMed: 21450292]
49. Asgari M, et al., In vitro fibrillogenesis of tropocollagen type III in collagen type I affects its relative fibrillar topology and mechanics. *Sci Rep*, 2017. 7(1): p. 1392. [PubMed: 28469139]
50. Karsdal MA, et al., The good and the bad collagens of fibrosis - Their role in signaling and organ function. *Adv Drug Deliv Rev*, 2017. 121: p. 43–56. [PubMed: 28736303]
51. Chapman MA, Pichika R, and Lieber RL, Collagen crosslinking does not dictate stiffness in a transgenic mouse model of skeletal muscle fibrosis. *J Biomech*, 2015. 48(2): p. 375–8. [PubMed: 25529136]
52. van der Slot-Verhoeven AJ, et al., The type of collagen cross-link determines the reversibility of experimental skin fibrosis. *Biochim Biophys Acta*, 2005. 1740(1): p. 60–7. [PubMed: 15878742]
53. Saini K, et al., Tension in fibrils suppresses their enzymatic degradation - A molecular mechanism for 'use it or lose it'. *Matrix Biol*, 2019.
54. West JB, et al., Structure-function studies of blood and air capillaries in chicken lung using 3D electron microscopy. *Respir Physiol Neurobiol*, 2010. 170(2): p. 202–9. [PubMed: 20038456]
55. Chapman MA, Meza R, and Lieber RL, Skeletal muscle fibroblasts in health and disease. *Differentiation*, 2016. 92(3): p. 108–115. [PubMed: 27282924]
56. Brandan E and Gutierrez J, Role of proteoglycans in the regulation of the skeletal muscle fibrotic response. *FEBS J*, 2013. 280(17): p. 4109–17. [PubMed: 23560928]

57. Fadic R, et al., Increase in decorin and biglycan in Duchenne Muscular Dystrophy: role of fibroblasts as cell source of these proteoglycans in the disease. *J Cell Mol Med*, 2006. 10(3): p. 758–69. [PubMed: 16989735]
58. Zhang G, et al., Genetic evidence for the coordinated regulation of collagen fibrillogenesis in the cornea by decorin and biglycan. *J Biol Chem*, 2009. 284(13): p. 8888–97. [PubMed: 19136671]
59. Pearson D and Sasse J, Differential regulation of biglycan and decorin by retinoic acid in bovine chondrocytes. *J Biol Chem*, 1992. 267(35): p. 25364–70. [PubMed: 1460033]
60. Zanotti S, et al., Decorin and biglycan expression is differentially altered in several muscular dystrophies. *Brain*, 2005. 128(Pt 11): p. 2546–55. [PubMed: 16183658]
61. Amenta AR, et al., Biglycan is an extracellular MuSK binding protein important for synapse stability. *J Neurosci*, 2012. 32(7): p. 2324–34. [PubMed: 22396407]
62. Theroux MC, et al., Dysmorphic neuromuscular junctions associated with motor ability in cerebral palsy. *Muscle Nerve*, 2005. 32(5): p. 626–32. [PubMed: 16025530]
63. Amenta AR, et al., Biglycan recruits utrophin to the sarcolemma and counters dystrophic pathology in mdx mice. *Proc Natl Acad Sci U S A*, 2011. 108(2): p. 762–7. [PubMed: 21187385]

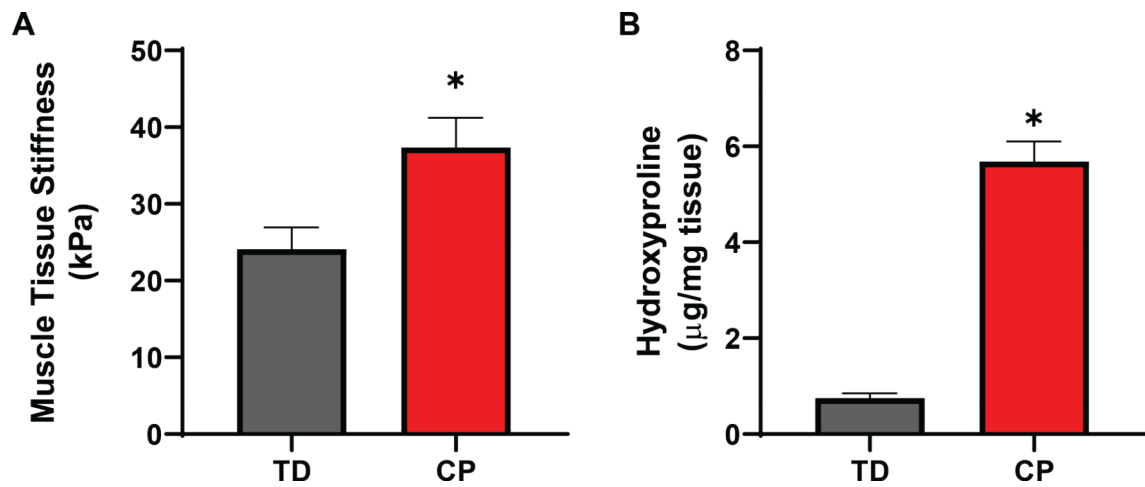


Figure 1: Differences in bundle stiffness and hydroxyproline between TD and CP muscles. **A)** CP patients showed significantly higher muscle bundle stiffness compared to TD (TD: 24.11 ± 2.73 ; CP: 37.37 ± 3.70 (kPa); $p < 0.05$). **B)** Hydroxyproline content, representing overall collagen, was markedly higher in patients with CP compared to TD (CP: 5681 ± 407 ; TD: 753 ± 93 ; $p < 0.0001$). N = 13 for both CP and TD samples.

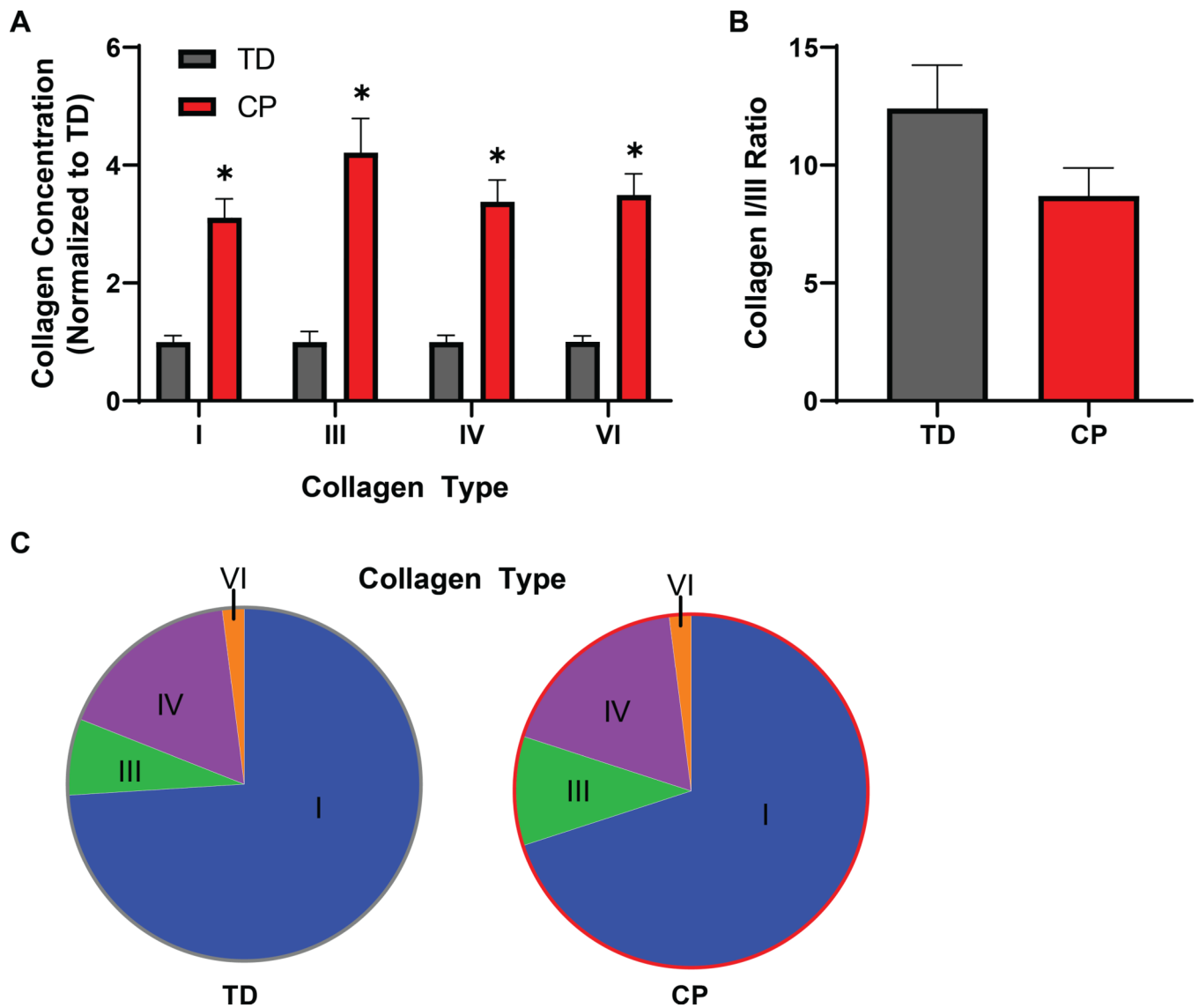


Figure 2: Increased levels of individual collagen types in CP. **A)** Collagen I, III, IV and VI levels measured by ELISA were increased significantly in children with CP compared with TD children. All collagens measured showed a 3–5 fold increase. **B)** Because collagen I had the lowest increase and collagen III had the highest fold increase, the I/III ratio was lower in CP samples, although this difference was not significant ($p=0.10$). **C)** Collagen I made up the largest proportion of collagen types measured (~70%) followed by collagen IV, III, and VI. Overall collagen proportions were not significantly changed with CP.

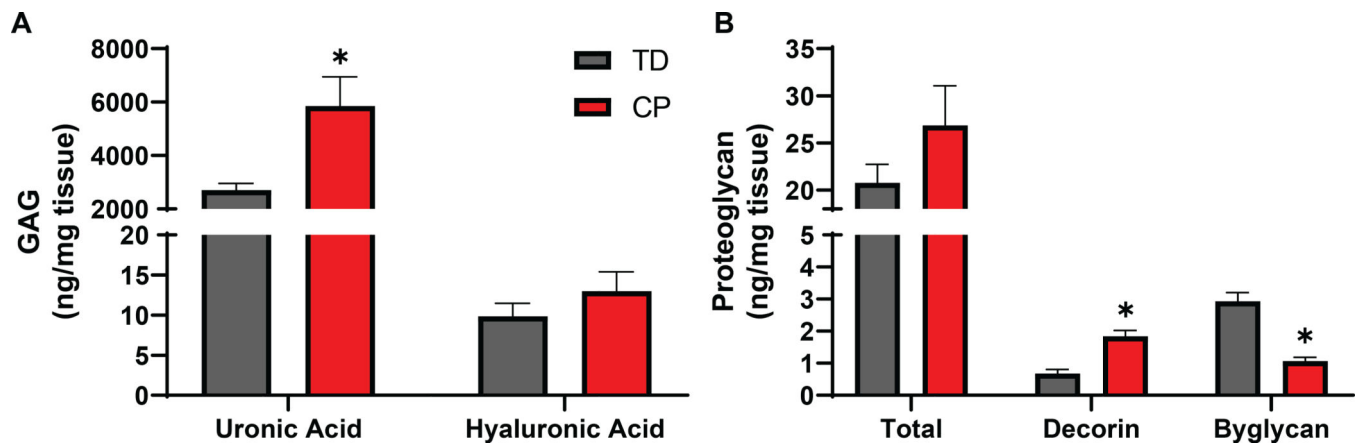
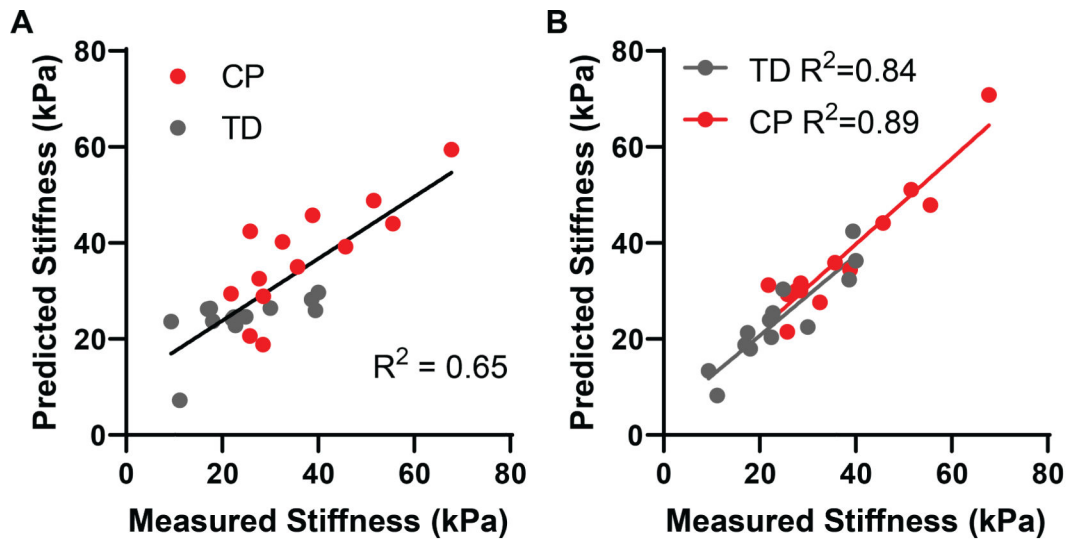


Figure 3:

Differences in GAGs and Proteoglycans in CP. **A)** Uronic acid present in all GAGs had an ~2-fold increase while hyaluronic acid was not significantly altered in CP compared to TD.

B) Overall proteoglycan content was not significantly altered in CP. SLRPs were differentially regulated with decorin demonstrating a 2.7 fold significant increase and biglycan a 2.7 fold significant decrease.



All Predicted Stiffness = $29 + 0.11[\text{COL1}] - 0.74[\text{COL3}] + 0.49[\text{PG}] - 5.85[\text{BG}]$

TD Predicted Stiffness = $-17.9 + 1.82[\text{HP}] + 1.82[\text{COL1}] + 0.74[\text{COL4}] + 1.37[\text{PG}] - 15.73[\text{BG}]$

CP Predicted Stiffness = $6.5 + 1.75[\text{COL1/3}] + 0.0043[\text{HPL}] + 0.45[\text{PG}] - 19.4[\text{BG}]$

Figure 4:

Stepwise linear regression of bundle stiffness on ECM biochemistry. **A)** Multiple stepwise linear regression performed on bundle stiffness for all 26 samples with 14 parameters of extracellular matrix components generated a model accounting for 65% of variance that included positive predictors collagen I (COL1), III (COL3), and total proteoglycan (PG) with biglycan (BG) as a negative predictor. **B)** Multiple stepwise linear regression on TD and CP samples separately resulted in better fitting models (TD: $R^2 = 0.84$; CP: $R^2 = 0.89$). Both included total proteoglycan and biglycan together with additional inclusion of positive predictors of hydroxylysyl pyridinoline (HP), collagen I and IV in TD and collagen I/III ratio and hydroxyproline (HPL) in CP.

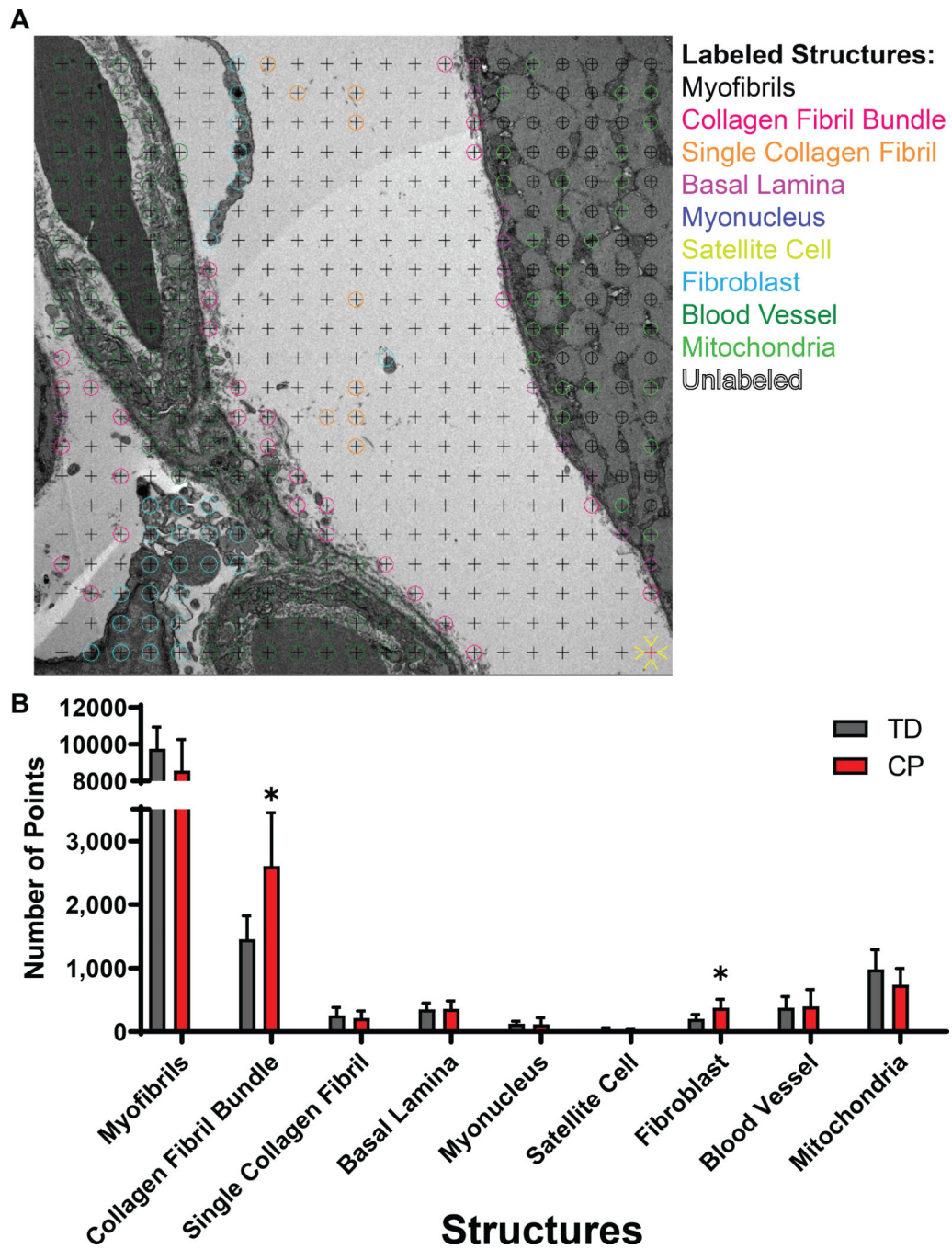


Figure 5: Stereological quantification of subcellular components of muscle tissue in CP and TD. **A)** Low magnification transmission electron micrograph of CP muscle shown with a 400-point stereological grid. Low and high magnification micrographs (n = 845) were analyzed for volume fraction of myofibrils, basal lamina, mitochondria, myonuclei, satellite cells, collagen fibrils in cables, single collagen fibrils, fibroblasts, and blood vessels, each shown in a different color (note that some components were only measured at high magnification and are identified here as examples). **B)** Stereological results comparing TD and CP muscle.

Note the significantly greater volume fraction of fibrils in cables and fibroblasts in CP muscle compared to TD.

Author Manuscript

Author Manuscript

Author Manuscript

Author Manuscript